Acta Montanistica Slovaca
ISSN 1335-1788
actamont.tuke.sk

Analyzing Pillar Strength and Behavior using Wolfram Mathematica code: Effects of Cracks, Size and Discretization

***Youcef CHEIKHAOUI*[1]*, *Hamza CHENITI*[1,2], *Ibtissem ZERIRI*[2], *Adel AISSI*[3], *Aissa BENSELHOUB*[2] *and* *Ali Ismet KANLI*[4]**

Authors' affiliations and addresses:
[1] National Higher School of Technology and Engineering, Department of mining, metallurgy and materials, 23005 Annaba, Algeria.
e-mail : y.cheikhaoui@ensti-annaba.dz

[2] Environmental Research Center, 23000 Annaba
e-mail: benselhoub@yahoo.fr

[3] University Mohamed Boudiaf, 28000 M'Sila, Algeria
e-mail: adel.aissi@univ-msila.dz

[4] Istanbul University-Cerrahpaşa, Istanbul. Department of Geophysical Engineering 34320 Avcilar Campus, Turkey
e-mail: kanli@istanbul.edu.tr

***Correspondence:**
Youcef Cheikhaoui, National Higher School of Technology and Engineering, Department of mining, metallurgy and materials, 23005 Annaba, Algeria
tel.: 213669501893
e-mail: y.cheikhaoui@ensti-annaba.dz

Acknowledgement:
I would like to thank everyone I had the pleasure of working with on this paper and related projects.

How to cite this article:
Cheikhaoui, Y., Cheniti, H., Zeriri, I., Aissi, A., Benselhoub, A. and Kanli, A.I. (2024). Analyzing Pillar Strength and Behavior using Wolfram Mathematica code: Effects of Cracks, Size and Discretization. *Acta Monstanistica Slovaca*, Volume 29 (3), 604-617

DOI:
https://doi.org/10.46544/AMS.v29i3.08

Abstract
The stability of fractured rock masses and the modeling of underground mining pillars necessitate a comprehensive understanding of behavioral models and mechanical properties. This study employs the Wolfram Mathematica code to investigate mining pillar reliability, specifically focusing on elucidating the influence of scale and shape on pillar strength. Drawing inspiration from methodologies in the existing literature, our approach is based on the Mohr-Coulomb theory and Griffiths's random field of rock strength. This study highlights the significance of shape, where pillar strength exhibits exponential growth with increasing width-to-height ratios. Beyond a critical value, strength surges, especially under elevated confining stress. Additionally, a critical mesh size significantly affects the weakest pillar behavior. Our results confirm the 'size effect,' wherein strength generally decreases with increasing pillar volume. Thus, strength decreases with rising volume until a threshold. Particularly noteworthy is the phenomenon observed in the presence of cracks; initially, an increase in mesh size leads to a decline in strength, corresponding to an increase in the number of cracks. However, this decline stabilizes beyond a critical mesh size, after which strength experiences a resurgence echoing behavior seen in the homogeneous case.
In this paper, the reproduction of the scale effect by an algorithm based on the Mathematica code was made to allow a probabilistic study to be carried out because of the random existence of discontinuities in nature – another hand to carry out stochastic modeling of fractures and its influence on the rock mass strength.

Keywords
Stability, Wolfram Mathematica, pillar strength, cracks, discretization, size effects.

Introduction

Pillars play a crucial role in underground mines, as they are essential for maintaining the stability and durability of excavations. In mines operating at considerable depths and experiencing high-stress levels, the stress fluctuations resulting from mining activities, coupled with the subsequent rock damage occurring throughout the mining process, can gradually weaken the strength around the pillar boundaries. Consequently, this deterioration may produce instability in the pillars and elevate the probability of activating these structural defects.

Hence, the stability of pillars and their failure characteristics assume a critical significance in ensuring mining safety. Extensive research endeavors spanning several decades have been dedicated to analyzing pillar failures and developing methods for evaluating their stability. Understanding the behavior of pillar systems when they fail serves as a foundational background for comprehending the impact of pillars on the stability of underground mine workings at both local and regional scales. This knowledge also aids in acknowledging the uncertainties inherent in pillar design and enables the effective management of associated risks (Liu et al., 2015)

The response of pillars to structural defects can differ significantly between mines and even within the same mine (Brady and Brown, 2004). This variability in behavior is primarily influenced by three key factors: the pillar shape, the characteristics of the surrounding rock, and the local geo-mechanical conditions. These factors collectively govern how pillars interact with and respond to potential structural defects, making their stability and susceptibility to defects unique to each mining operation. Also, the observed scale effect in can be attributed to the growing presence of discontinuities within the rock mass as its volume increases. Weibull, 1951 corroborated this phenomenon by establishing that as the probability of defects increases, the mechanical properties, including strength and hardness, proportionally decrease with size. Thus, the implications of the scale effect on the determination of characteristic values for the mechanical properties of rock masses hold paramount importance, particularly in the context of mining structures, risk management associated with resource exploitation, and land planning. A comprehensive understanding of this phenomenon is essential for informed decision-making and robust engineering practices in these domains.

The strength of pillars demonstrates a power law relationship, resulting in a decrease in strength as the volume of the pillar increases. Additionally, a significant shape effect is observed (Gao et al., 2018), indicating that the strength values of the pillars rise with higher shape ratios (w/h). This emphasizes the pivotal role of the pillar's aspect ratio in determining its overall behavior (Cheikhaoui et al., 2021; Martin and Maybee, 2000; Salamon, 1996)

The scale effect on pillar strength is attributed to the presence of various micro-fractures and defects, such as cracks within the pillar. This decrease in strength with increasing rock specimen size is typically associated with an augmented number of defects at smaller scales (centimeters) and the influence of rock mass structure at larger scales (meters to decimeters), as noted by Alejano et al. (2015).

Furthermore, an exponential increase in strength is observed with an increase in the w/h ratio. The size effect consistently manifests, with smaller volumes exhibiting higher strength values. Notably, strength rapidly approaches a maximum value at a critical w/h ratio. A rock mass's strength is often characterized by a constant cohesive component and a component dependent on normal stress or confinement. Consequently, for pillars with $w = h$ or ratios greater than 1, strength should increase as the confining stress rises, as discussed by Youcef Cheikhaoui et al. (2021).

Modeling serves the purpose of mathematically representing physical phenomena, with the model designed to accurately capture the fundamental intrinsic characteristics of the phenomenon under investigation. Once created, the model is subjected to execution and validation within a computerized environment. In our study, we have opted to leverage the Wolfram Mathematica code (Wolfram Research, Inc., 2023), a widely recognized scientific computing software. Utilizing the Mathematica language empowers us with greater control by enabling the programming of custom codes that can elucidate the influence of scale and shape on pillar strength. Our approach draws inspiration from analytical methods presented in the existing literature.

To comprehensively address the effects of scale and shape in rock masses, particularly in the context of mining pillars, we consider the following key factors:

- The influence of volume (V).
- Incorporation and assessment of the impact of a family of discontinuities, including aspects like dip, spacing, and mechanical properties.
- Examination of the behavior of the rock matrix, encompassing parameters such as cohesion and internal friction angle.
- Consideration of the influence of discretization, which involves the meshing of the pillar (Yoshinaka et al., 2008).

Our primary objective is to construct a 2D model that faithfully represents a mining pillar with well-defined dimensions, encompassing width and length. In reality, a pillar comprises various rock fractions, each possessing distinct geo-mechanical properties such as compressive strength, cohesion, and internal friction angle, in addition

to the presence of discontinuities characterized by geometric properties like angle and width. To emulate this complexity, our model is divided into discrete meshes, each corresponding to a specific rock fraction and inheriting its respective geo-mechanical properties. This approach allows us to investigate the intricate interplay of factors influencing pillar behavior comprehensively.

As a case study, we use data from the Chaabet El-Hamra underground mine in Algeria (Fig.1), and the mine depth varies between 106.5 m and 112 m. In the room and pillar mining method employed, the pillars generally take on a square shape with variable dimensions based on the adopted extraction ratio, which ranges between 72% and 84%.

Previous mechanical tests were conducted to determine the uniaxial compression strength of the zinc rock, yielding a range of values between 40.4 and 159.9 MPa. The Chaabet El-Hamra deposit is located approximately 250 Km South-East of Algiers and 50 kilometers south of Setif, specifically within the Chouf-Bouarket area, positioned 4.5 Km from Ain-Azeland and 12 Km South-East of the Kherzet Youssef mining complex, as depicted in Figure 01. Using the WGS 1984 coordinates scheme, its geographical coordinates fall between 35° 45'N and 35° 48'N latitude and 5° 31' E and 5° 32' E longitude.

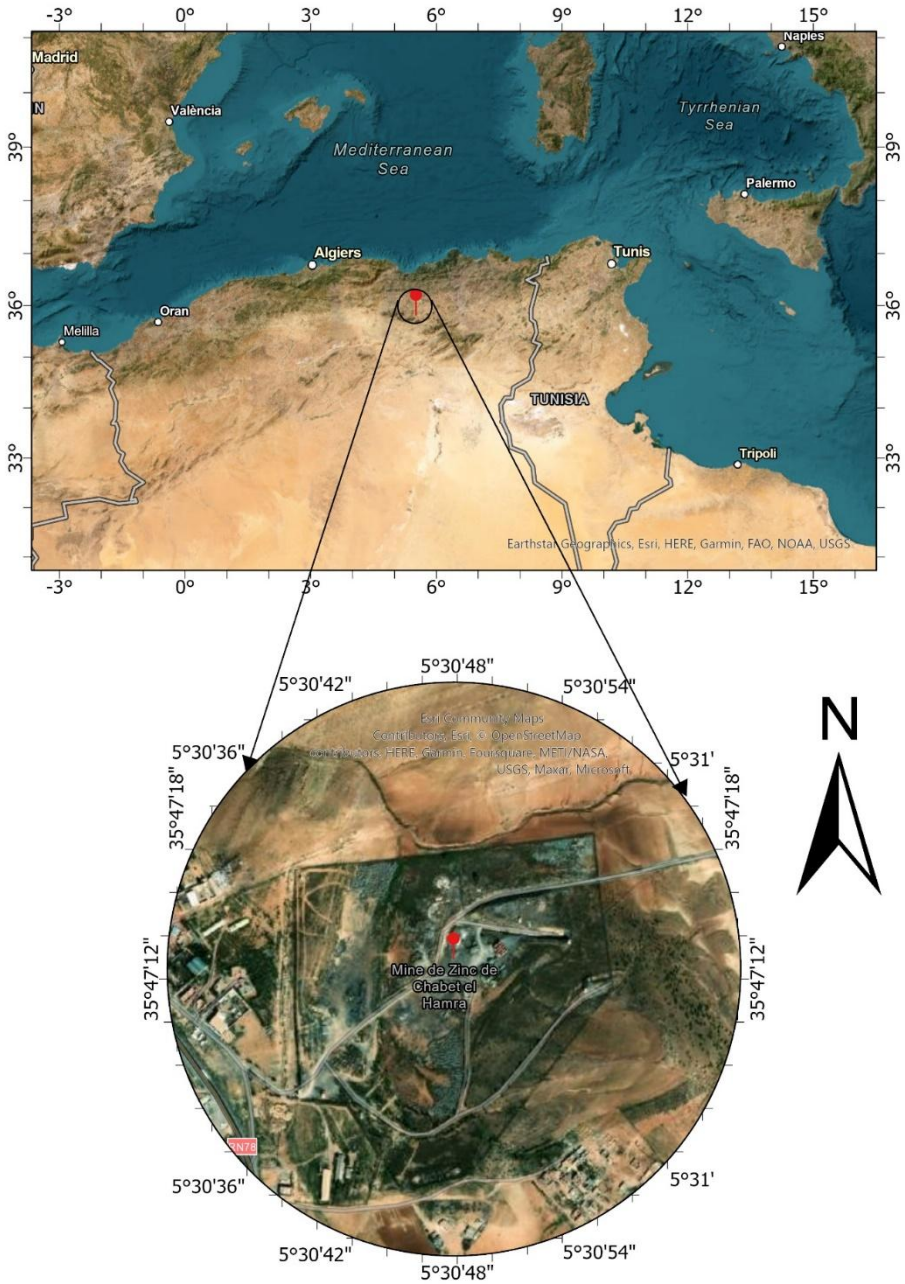

Fig. 1. Geographical location of Chaabet El-Hamra underground mine

Material and Methods

The structural response of a pillar to mining-induced loading is influenced by several factors, including the properties of the rock material, geological structure, the absolute and relative dimensions of the pillar, and the nature of surface constraints imposed by the surrounding country rock. Lunder & Pakalnis (1997) delineated the progressive stages of pillar degradation in terms of deformation modes, as depicted in Fig. 2 (A). Initial indications of rock stress may manifest as localized shear failure, often associated with re-entrant geometries (Fig. 2a). The formation of surface spalls (Fig. 2b) represents a more extensive failure, indicative of stress conditions that meet the criteria for fracture initiation and substantial rock damage within a significant portion of the pillar. The pillar is considered to have partially failed at this stage, although its core remains intact. Elevated levels of stress contribute to the accumulation of damage through the initiation and propagation of internal cracks, along with the interaction between these families of cracks (Fig. 2c). When the friction between the fully developed population of cracks is maximized (Fig. 2d), the pillar reaches its peak strength but is considered mechanically failed. This model of progressive pillar failure aligns with the micromechanical modeling of pillar loading reported by (Diederichs, 2002), which observed the gradual formation of cracks and the localization of shear strain.

The propagation of discontinuities, whether occurring gradually or rapidly, is governed by a load ratio mechanism. This mechanism is based on the principle that the load-bearing capacity of cracked portions weakens, which increases the load demand on the uncracked sections, potentially pushing them beyond their strength limits. It is important to note that this process does not necessarily lead to the immediate collapse of the pillar or the failure of the entire operation. Instead, it results in a redistribution of stress within the pillar, characterized by the presence of a fractured segment, which may still be compatible with a stable but compromised state. This is particularly true when the pillars are sufficiently spaced apart, and the overall safety coefficient remains high, preserving the system's overall stability.

Three distinct mechanisms of damage have been identified by (Maybee, 2000), based on relative criteria pertaining to the speed of damage, independent of the specific modes of fracture:

1- Progressive cracking characterized by the gradual propagation of fractures.
2- Sudden cracking often controlled by geological structures, particularly when the pillar's positioning is unfavorable in relation to discontinuities (commonly referred to as slip bursts).
3- Sudden damage caused by rock bursting, known as pillar bursts. Typically, progressive damage results in significant pillar deterioration over several years (Ma et al., 2012).

In contrast, sudden discontinuities occur rapidly, on the scale of seconds, and are exceptionally challenging to predict due to the absence of discernible precursor signs (Zipf and Mark, 1997).

1. The random field of rock strength

Griffiths et al. (2002) and Griffiths & Fenton (2004) introduced a method (Fig.2 (B)) that addresses the impact of rock strength variability on the overall compressive strength of rock pillars, commonly used in mining and underground construction. This technique integrates elastoplastic finite element analysis with random field theory within a Monte Carlo framework. Rock strength is primarily characterized by its unconfined compression strength or "cohesion," following the Tresca plasticity criterion (elasto-perfectly plastic). The spatial correlation length describes the distance over which spatially random values tend to exhibit correlation in the underlying Gaussian field. A high correlation length indicates a smoothly varying field, while a low value suggests greater irregularity.

The local mean subdivision method is employed to simulate the random field of spatially varying rock strength. Values representing the random field of rock compression strength are generated through Monte Carlo simulation. It is important to note that this study focuses on plane deformation pillars with square dimensions within the analysis plane. Fig. 3 illustrates a typical finite element mesh, where each element is assigned a distinct cohesion value based on the underlying lognormal distribution.

The principles outlined in Griffiths' work provide valuable insights into representing strength variability and spatial correlation length. These insights are particularly useful for introducing the characteristics of pillar meshes into the modeling process in the initial stages.

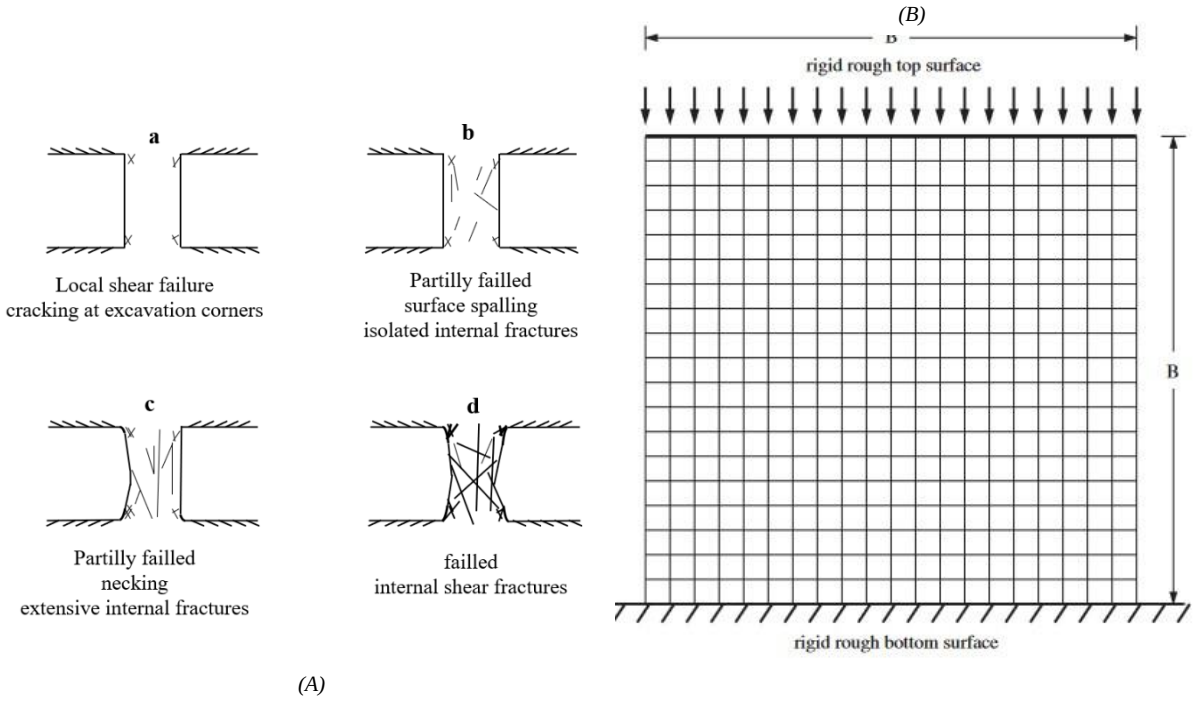

Fig. 2. (A) Schematic illustration of the evolution of fracture and failure in a pillar in massive rock (Lunder & Pakalnis, 1997) .(B) Mesh used for Finite Element Analyses(Griffiths & al., 2002), Modified by authors.

2. Estimating pillar strength

The first empirical formulas for pillar design were developed for coal mines and are, therefore, primarily applicable to soft rocks. These formulas minimize the scale effect by testing cubic samples with a 1-meter side and experimentally determining the uniaxial compression strength (UCS) of these samples. For several coal mines using room-and-pillar methods, Bieniawski (1968) proposed a formula to calculate the strength of coal pillars:

$$\sigma_p = C + M\,(w/h) \tag{01}$$

Other formulas have been developed for hard rocks, incorporating a scale factor to account for a reduction in the uniaxial compressive strength of the intact rock, which typically ranges between 40% and 80%. This adjustment is necessary because the scale factor considered in formulas for soft rocks is not directly applicable to hard rocks. Several of these formulas are derived from the power formula of Salamon and Munro:

$$\sigma_p = kh^a w^b \tag{02}$$

They have empirical equations of pillar strength obtained by back-analysis.
The study of the literature (Tab.01), through the use of the Galvin formula:

$$\sigma_p = kV^{\alpha}\,(w / h)^{\beta} \tag{03}$$

A new analytical formula developed by Cheikhaoui et al. (2021) uses Weibull's parameters to account for the effects of scale (size and shape) and incorporates probabilistic notions to evaluate the risk of failure. This formula (04) allows for the assessment of mine pillar conditions without the need for pillar-level experiments.

$$\sigma_p = \sigma_0 ln(1/P_s)^{-\alpha}\,.(w / h)^{\beta}.V^{\alpha} \tag{04}$$

Such as:

α= -1/m

β= $\ln(V_0^{1/m})/\ln(W_{ep}/H_{ep})$

where:

V_0: Specimen volume (m^3).

V: pillar volume (m^3).

W_{ep}/H_{ep}: Ratio of the shape of the specimen.

w/h: Pillar shape ratio.

Weibull's parameters

m: represents material parameter characterizing the dispersion of defects within the material,

σ_0: represents the stress associated with a probability of failure of 37% of the test specimens (Mpa).
P_s: probability of survival.

For coal, the suggested values are $\alpha \in [-0.2; 0]$ and $\beta \in [0.5; 1]$. These values are consistent with those typically found using Weibull parameters. In contrast, for Zinc Ore, the values of α and β are larger because the rock is harder than coal.

Tab. 1. Coefficients of the power law defined by equation 2 after (Salamon, 1996)" modified'

Autor	R_0 [Mpa]	α	β	Comment	Rock type
Zern (1928)	-	0	0,5	-	-
Greenweld (1939)	19.3	-0,11	0,72	Large-scale in situ testing	Coal
Holland et Goddy (1957)	-	-0,166	0,83	Laboratory tests	Coal
Salamon et Munro (1966)	7.2	-0,066	0,59	Retroanalysis	Coal
Wagner (1967)	11.0	0	0,5	Large-scale in situ testing	Coal
Bieniawski (1967)	4.5	0	0,5	As reported by van Heerden (1975)	Coal
van Heerden (1975)	13.3	0	0,5	Large-scale in situ testing	Coal
Galvin et al. (1996)	7.2	-0.067	0.59	As reported by Salamon et Munro (1966)	Coal
Cheikhaoui et al., 2021	-	-0.086	0.45	Laboratory tests as reported by Galvin et al. (1996)	Coal
Cheikhaoui et al., 2021a	23.6	-0.4	5.1	Laboratory tests	Zinc Ore

3. Modeling approach

Wolfram Mathematica, a comprehensive computational software developed by Wolfram Research since 1988, is extensively utilized in scientific research for algebraic computations and custom program development. The software's development began in 1986, culminating in its first release in 1988. Mathematica is compatible with multiple platforms and supports a wide array of mathematical operations. Furthermore, Wolfram Research has established an intelligent online resource, Wolfram Alpha, which integrates functionalities derived from Mathematica and is available to users at no cost (Wolfram Research, Inc., 2023).

The primary objective of this study is to develop a simple yet robust analytical model that effectively captures the effects of scale and shape. Once a satisfactory model is achieved, it will be systematically compared with alternative models to define its scope of applicability and refine any parameters or choices that may initially appear arbitrary. Our initial focus is on analyzing outcomes related to the volume effect, given its critical importance in understanding scale effects. To determine pillar strength using the model, we will develop calculation algorithms that incorporate geomechanical parameters. The model will be executed in multiple iterations to produce statistical distributions, including the average and standard deviation. Additionally, geotechnical simulation software will be employed to assess the pillar's strength and behavior.

In this study, we concentrate on the pillars within underground mines, where compressive strength is a critical parameter for stability assessments, particularly given that these pillars are situated in fractured rock environments where stability must be rigorous (Cheikhaoui et al., 2021; Medhurst and Brown, 1998). The initial modeling phase involves representing the mining pillar in a two-dimensional framework. Specifically, the pillar is modeled as a matrix of dimensions (n x m), where n represents the number of vertical meshes corresponding to the pillar's height h, and m denotes the number of horizontal meshes aligning with the pillar's width w. Each cell in this matrix represents a discrete volume unit of the pillar, incorporating N estimates. The average strength value of these estimates is then computed to construct the strength-volume variation curve.

To estimate the strength of the pillar, we rigorously evaluate and implement several algorithms. The algorithm that yields the most favorable results is presented herein. This approach is grounded in a robust theoretical framework, introducing the concept of shear planes where structural failures are likely to occur. We perform a virtual plane sweep, calculating shear strength at each step, with the minimum strength value indicating the overall pillar strength (Fig. 3). The algorithm, developed using Mathematica, is based on the Mohr-Coulomb theory and assesses the potential for shear failure at each point within the pillar. For a cracked pillar, the algorithm specifically accounts for the influence of crack orientation on strength.

- **Mohr-Coulomb's theory**

According to Mohr-Coulomb theory, the failure of a rock subjected to normal stress takes the form of shearing. The shear strength of a rock is a function of the internal friction angle and the cohesion at the shear plane. The shear strength is linearly related to the normal stress:

$$\tau = \sigma n.\tan(\theta) + c \quad (05)$$

τ: Shear stress
θ: Internal friction angle
c: Cohesion
σ_n: Normal stress relative to the sliding plane

- **Stability calculation**

The stability of the pillar depends on its shear strength and the driving force applied at the shear plane. If the shear strength is greater than the driving force, it is a case of stability. The stress on the pillar is divided into two components at the shear plane: normal stress and tangential stress.

$$\sigma = \sigma_n + \sigma_\tau \quad (06)$$

Normal stress $\sigma_n = \sigma \cos\alpha$ (07)

Tangential stress $\sigma_\tau = \sigma \sin\alpha$ (08)

Thus $\sigma = \sigma \cos\alpha + \sigma \sin\alpha$ (09)

α: Shear plane angle

So the shear strength: $\tau = \sigma \cos\alpha \tan(\theta) + c$ (10)

The driving constraint: $\sigma_\tau = \sigma \sin\alpha$ (11)

If $\tau > \sigma_\tau$ we are in the stable case otherwise, the pillar breaks by shear

We have $\sigma \cos\alpha \tan(\theta) + c > \sigma \sin\alpha$ so: $\sigma < c / \sin\alpha - \cos\alpha \tan(\theta)$ (12)

Thus $\sigma_{max} = c / \sin\alpha - \cos\alpha \tan(\theta)$ (13)

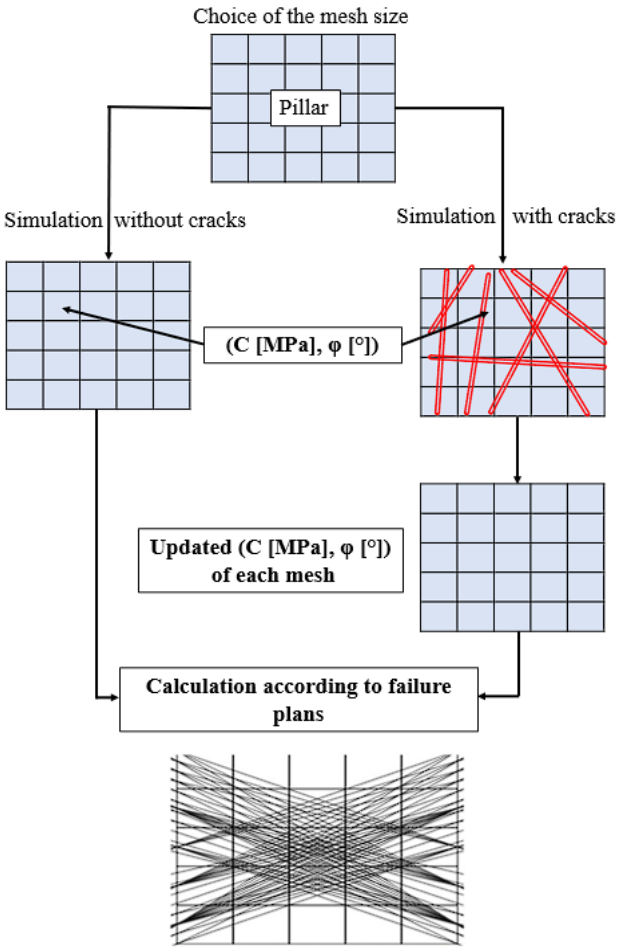

Fig.3 Diagram showing the simulation principle for a case study (underground pillar)

4. The Spatial Distribution of Mechanical Properties within the Mining Pillar

In this methodology, we utilize the Hoek-Brown criterion (Hoek and Brown, 1997), a well-established physical model that relates the properties of a rock mass to the mechanical properties of its intact rock components, to calculate the maximum stress. This criterion allows us to determine equivalent cohesion and internal friction angle values for each element within the mining pillar. It is essential to recognize that the construction of the pillar significantly influences its mechanical behavior. As a result, the pillar's strength is intricately associated with the spatial distribution of mechanical properties throughout its structure.

A pressing question arises: How can we effectively distribute strength properties across the entire volume of the pillar while accounting for scale effects in the overall strength calculations?

In the following sections, we detail our approach to generating representative strength values, which is crucial for refining our algorithm. We start by modeling the mining pillar within a two-dimensional (2D) framework, represented as a matrix with dimensions (n x m), where n denotes the number of mesh divisions along the pillar's height h, and m represents the number of mesh divisions along its width w. Each cell in this matrix represents an elementary volume within the pillar. We then populate this matrix with characteristic cohesion values and the angle of internal friction. The Hoek-Brown criterion, which provides a physical basis for these values, is utilized to assign cohesion and friction angle values to each mesh element. This distribution ensures that our model accurately captures the essential strength characteristics of the pillar.

Results

1. Geomechanical Classification of the Chaâbet El-Hamra Massif

This study draws upon data from the ENOF (National Company of Non-Ferrous Mining Products and Substances) and operational plans pertaining to the upper section, specifically the upper beam, of the Chaabet El-Hamra mine. Figure 4a presents the operational layout, which includes profiles 1 through 10 within this upper mine section. This detailed plan is instrumental in identifying various mine panels and distinguishing between exploited and unexploited zones.

An examination of the cross-sectional face at profile 9, block P 5/1, reveals a distinct family of fractures, prominently featuring seven discontinuities -representing the maximum observed occurrence- within a confined 1 m² area. These fractures belong to the N130-70NE family and exhibit variable spacing, ranging from 10 cm to 30 cm. They consistently display light roughness with unaltered wall conditions and are filled with cemented calcite, with thicknesses varying between 2 mm and 5 mm.

- **Rock Quality Designation RQD**

There are alternative methods that prove to be very useful for estimating the RQD index when no geological drilling is available. (Hudson et al., 1972) established a relationship between the spacing of joints (λ [joints/meter]) determined from surface measurements of the exposed rock mass and the RQD index.

$$RQD = 100\, e^{-0.1\lambda}(0.1\,\lambda+1) = 100\, e^{-0.7}(0.7+1) = 84 \quad (14)$$

- **Rock Mass Rating RMR Classification**

Table 2. RMR classification for the Chaabet El-Hamra mine

A			Value	Rating
A1	1: Uniaxial compressive strength (MPa)		50-100	7
A2	2: Rock Quality Designation RQD		84	17
A3	3: Discontinuity spacing (mm)		200-600	10
	4: Conditions of Discontinuities	Continuity (m)	3-10	3
		Opening (mm)	<5	1
		Roughness	Slightly rough	3
		Filling (mm)	<5	4
		Degree of alteration	No	6
A5	5: Groundwater		Dry	15
B	Adjustment according to the joint's orientation		Tunnel and	-5
RMR =	**61**			
RMR'89 = A1+A2+A3+A4+15 =	66			
Description: **Good Rock**	Rock Class: II			

- **Q-Barton Classification**

Table 3. Q-Barton classification for the Chaabet El-Hamra mine

Parameters	**Rating**
RQD	84
J_n	2
J_r	3
J_a	0.75
J_w	1
SRF	1
Q-system	**67.2**
Rock class	**Good**

- **Geological Strength Index (GSI)**

GSI= RMR'89 – 5 if RMR $\geq$ 23 else GSI= 9log Q' + 44 (15)

GSI= 61 Rock class: Good

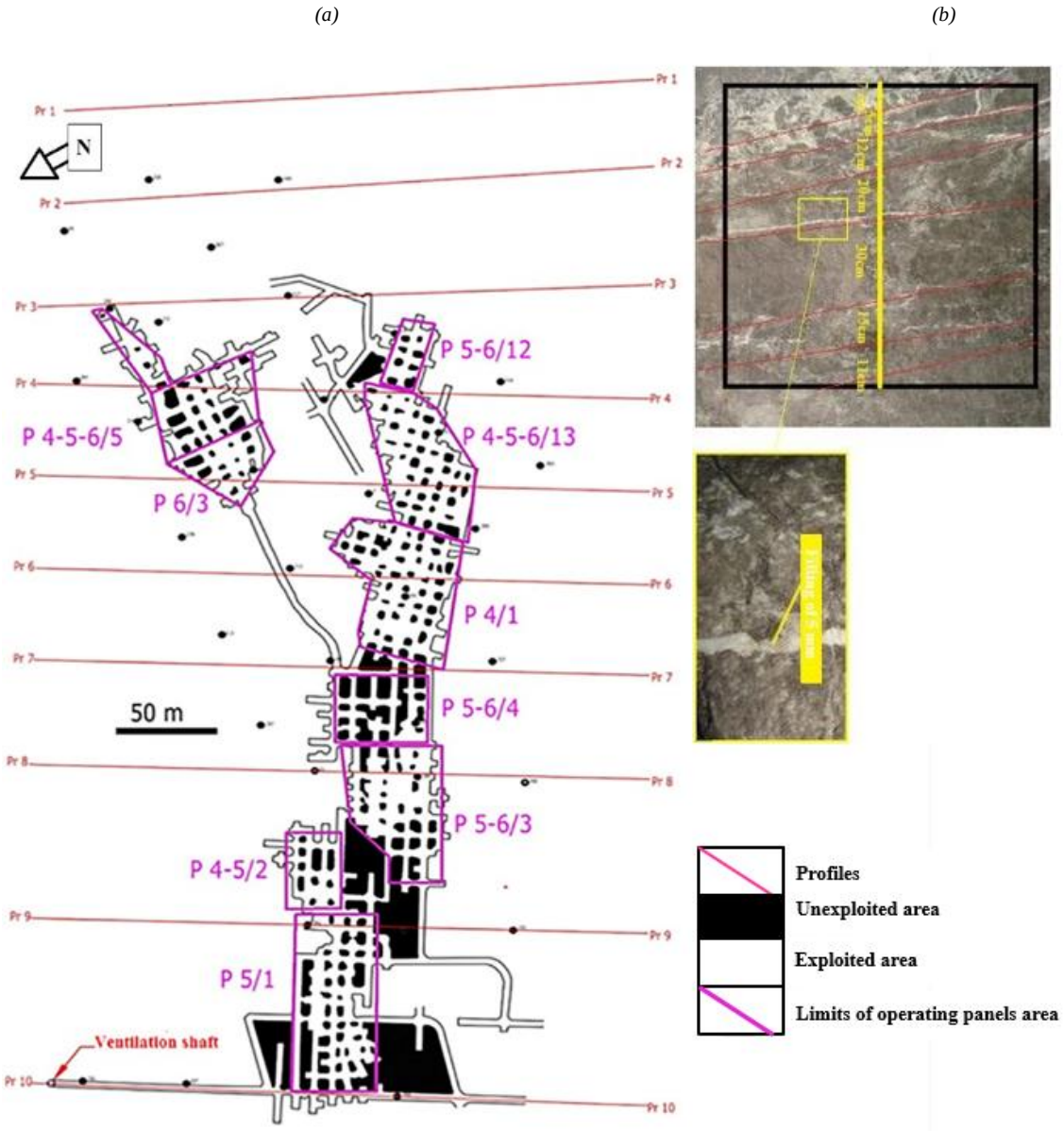

Fig 4. (a). Exploitation plan for the upper section - upper shaft of the Chaabet El-Hamra (Y Cheikhaoui et al., 2021). *(b). In-situ measurements of discontinuities on a pillar*

The results of this modeling, as illustrated in Fig.5 (a to f) below, have led us to draw three key conclusions: the volume effect, the shape effect, and the impact of increasing mesh size. These insights are derived from scenarios when we draw upon established principles in rock mechanics (Cundall et al., 2008; Greminger, 1982), wherein the cohesion and internal friction angle for each mesh element within the pillar are estimated using the Hoek and Brown classification and the Mohr-Coulomb criterion.

2. Size effects

For a square pillar with width and height $w = h = 3$ meters and a constant mesh number of 16 per side, each mesh's behavior is evaluated according to the Hoek-Brown criterion, applied to the specific conditions of the Chaabet El Hamra mine. The Hoek-Brown parameters are computed using Mathematica, based on input data including a crack spacing of 0.2 meters with a standard deviation of 0.1 meters, a crack dip of 70° with a standard deviation of 3°, and joint quality values from the Hoek-Brown classification. The Joint Compression Strength (JCS) is set to 14 for an intact rock type, with a material constant =24 and an average compressive strength of the intact rock at 84.88 MPa.

Figure 5(d) demonstrates the crack generation process within our algorithm, where cracks are randomly generated based on the specified standard deviations. Additionally, we quantify the number of cracks present in each mesh within the pillar.

This dataset enables us to determine the behavior of each mesh, which is then characterized using the Mohr-Coulomb criterion. Parameters such as cohesion (in MPa) and internal friction angle (in degrees) are specified, as shown in Table 4.

Table 4. Cohesion Matrix and Local Angle of Friction (C [MPa], φ [°]) for a Pillar Modeled with Mathematica.

{2.81 ,39.17}	{2.81 ,39.17}	{2.69 ,38.4}	{2.81 ,39.17}	{2.81 ,39.17}	{2.81 ,39.17}	{2.73 ,38.70}	{2.73 ,38.70}	{2.81 ,39.17}	{15.80 ,50.22}
{2.81 ,39.17}	{2.99 ,40.27}	{2.73 ,38.70}	{2.73 ,38.70}	{2.81 ,39.17}	{2.99 ,40.27}	{2.99 ,40.27}	{2.81 ,39.17}	{2.81 ,39.17}	{2.99 ,40.27}
{2.73 ,38.70}	{2.81 ,39.17}	{2.81 ,39.17}	{2.73 ,38.70}	{2.73 ,38.70}	{2.81 ,39.17}	{2.81 ,39.17}	{2.81 ,39.17}	{2.99 ,40.27}	{2.99 ,40.27}
{2.81 ,39.17}	{2.81 ,39.17}	{2.81 ,39.17}	{2.81 ,39.17}	{2.81 ,39.17}	{2.81 ,39.17}	{2.81 ,39.17}	{2.73 ,38.70}	{2.81 ,39.17}	{2.99 ,40.27}
{2.73 ,38.70}	{2.81 ,39.17}	{2.81 ,39.17}	{2.73 ,38.70}	{2.81 ,39.17}	{2.81 ,39.17}	{2.99 ,40.27}	{2.81 ,39.17}	{2.73 ,38.70}	{2.81 ,39.17}
{2.81 ,39.17}	{2.73 ,38.70}	{2.99 ,40.27}	{2.81 ,39.17}	{2.73 ,38.70}	{2.73 ,38.70}	{2.81 ,39.17}	{2.81 ,39.17}	{2.81 ,39.17}	{2.81 ,39.17}
{2.81 ,39.17}	{2.73 ,38.70}	{2.81 ,39.17}	{2.81 ,39.17}	{2.81 ,39.17}	{2.81 ,39.17}	{2.81 ,39.17}	{2.81 ,39.17}	{2.81 ,39.17}	{2.81 ,39.17}
{2.73 ,38.70}	{2.73 ,38.70}	{2.81 ,39.17}	{2.81 ,39.17}	{2.73 ,38.70}	{2.81 ,39.17}	{2.73 ,38.70}	{2.81 ,39.17}	{2.73 ,38.70}	{2.73 ,38.70}
{2.81 ,39.17}	{2.73 ,38.70}	{2.73 ,38.70}	{2.99 ,40.27}	{2.81 ,39.17}	{2.81 ,39.17}	{2.81 ,39.17}	{2.81 ,39.17}	{2.81 ,39.17}	{2.81 ,39.17}
{2.81 ,39.17}	{2.73 ,38.70}	{2.69 ,38.42}	{2.81 ,39.17}	{2.73 ,38.70}	{2.81 ,39.17}	{2.73 ,38.70}	{2.81 ,39.17}	{2.81 ,39.17}	{2.73 ,38.70}

3. Shape effect

Our investigation into the shape effect, systematically generated using the Mathematica algorithm, reveals a significant trend illustrated in Figure 5(b). The curve demonstrates an exponential increase in strength as the width-to-height ratio (w/h) rises. A critical observation is that strength increases markedly beyond a specific w/h threshold. This behavior is consistent with fundamental principles of rock mass strength (Alonso et al., 2012; Brady and Brown, 2004), which include a constant cohesive component and a stress-dependent component influenced by confinement. Therefore, for pillars with w/h ratios greater than 1, we expect strength to increase proportionally with the confining stress. This pattern mirrors the behavior of rock masses, where strength is

governed by both a constant cohesive element and a component that varies with stress. Consequently, as w/h ratios exceed 1, a corresponding rise in strength can be anticipated due to the increased confining stress.

4. **Mesh effect**

The choice of mesh size is crucial in determining the behavior of the pillar. Therefore, it is essential to thoroughly investigate the Mesh Effect for every new estimation of pillar strength. As illustrated in Fig. 5(c), a critical mesh size exists that leads to the most pronounced manifestation of weak behavior, ultimately resulting in the lowest observed pillar strength.

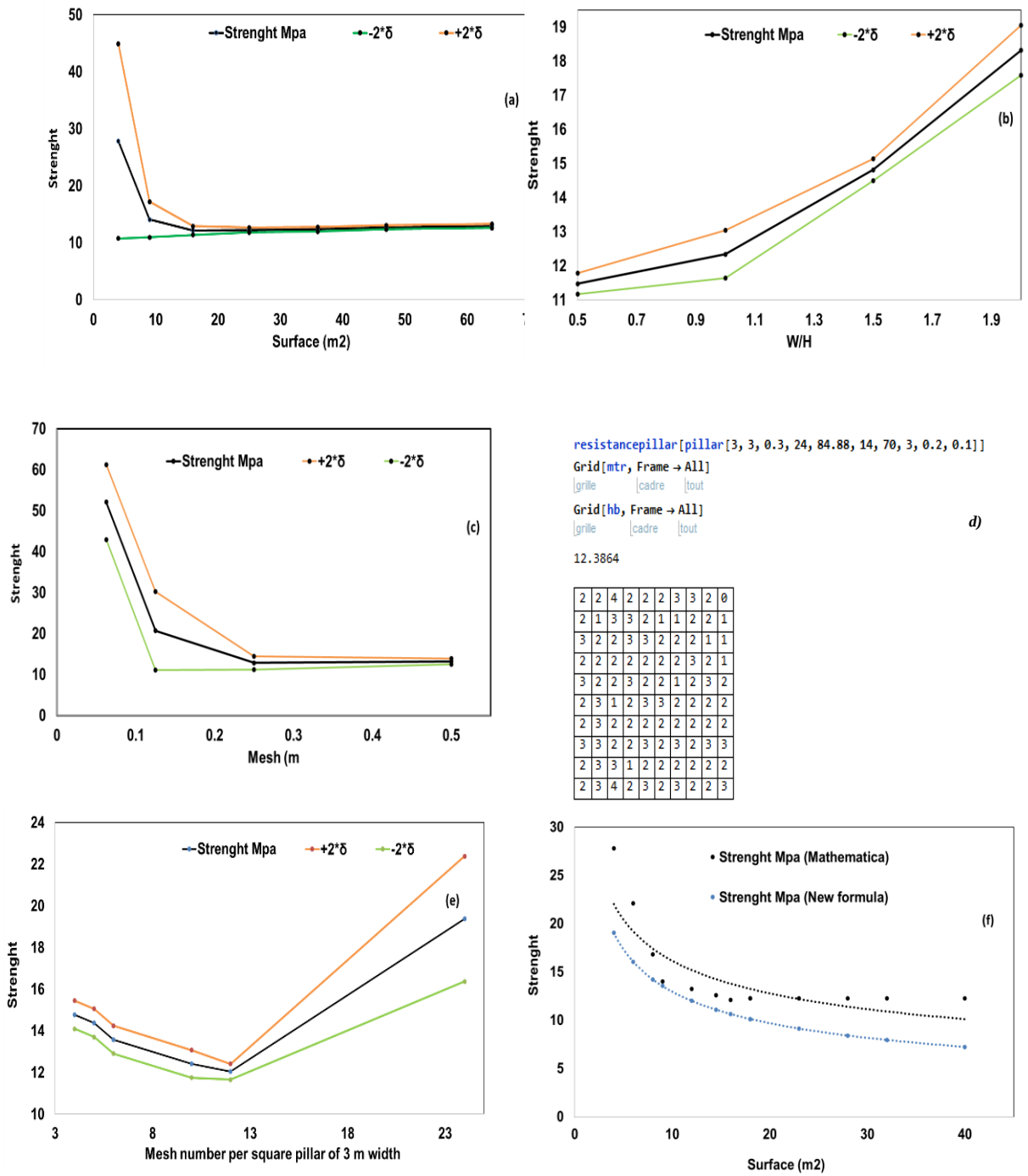

Fig 5. (a). Volume effect, case of 70° cracks spaced 0.2 m apart, constant number of meshes =16 for each side, w/h=1, (b). Shape effect, case of 70° cracks spaced 0.2 m apart, 10 meshes, pillar with 3 m sides, (c). Mesh effect, case of 70° cracks spaced 0.2 m apart, pillar with a side length of 3 m, (d). Representation of the code line and the discontinuity matrix in a pillar modeled by Mathematica, (e). Mesh effect, case of 70° cracks spaced 0.2 m apart, pillar 3 m long, square shape w/h=1, (f). Strength curves by Mathematica and the new formula using Weibull parameters.

Discussion

Our algorithm, implemented in Mathematica, produced logical strength values for both intact and cracked pillars. We analyzed these values under two conditions: one with a constant number of meshes across varying volumes and another with a fixed mesh size, resulting in a proportional increase in the number of meshes with volume. In accordance with existing literature (Wang et al., 2016), our results revealed a trend of decreasing strength with increasing volume, known as the 'volume effect.' Notably, there is a critical threshold beyond which this decreases levels. Based on the Mohr-Coulomb theory, our algorithm evaluates the potential for shear along each virtual failure plane within the pillar. For pillars with cracks, the strength inherently depends on the shear plane's angle.

Moreover, we observed that strength generally remained stable as volume increased when the mesh size was fixed. However, increasing the number of meshes with volume - while keeping mesh size constant - did not replicate the scale effect or account for the increasing number of discontinuities. Our findings also indicated that strength decreased with volume up to a certain threshold, beyond which further decreases were no longer observed. Additionally, the density of cracks had a notable impact on strength values, with smaller crack spacing (1 m) resulting in lower strength compared to larger spacing (1.5 m).

When applying the Hoek and Brown approach, we again observed that strength remained relatively constant as volume increased with a fixed mesh size, regardless of crack presence. This observation reinforces our earlier findings on the influence of fracture density on strength values. We found that strength increased as the width-to-height ratio (w/h) rose, both in homogeneous conditions and in the presence of cracks. This trend was consistently observed with the Hoek and Brown approach, as illustrated in Fig. 5(e).

Our investigation of the discretization effect showed that strength increased with larger mesh sizes. However, this came at the cost of a reduced number of meshes within a given volume. This reduction occurred because our strength calculation method relies on planes centered within these meshes. As the number of meshes decreased, the orientation of these planes tended to align with the internal friction angle, which represents the angle associated with the highest strength value (Fig. 5(e)).

Particularly notable is the behavior observed in the presence of cracks: initially, an increase in mesh size resulted in a decline in strength, which was correlated with an increase in the number of cracks. However, this decline stabilized beyond a critical mesh size, after which strength increased, mirroring the behavior seen in homogeneous conditions.

Analytically, we derived a strength formula utilizing Mathematica software under the assumption of a square pillar ($w/h = 1$): $R_p = 35.17\ V^{-0.338}$ (16)

Additionally, according to the strength formula using Weibull parameters, maintaining the assumption of a square pillar ($w/h = 1$): $R_{p(Ps=0.97)} = 34.09\ V^{-0.42}$ (17)

A comparison of the resulting strength curves for the square pillar case ($w/h = 1$) reveals a notable convergence in strength estimation, as shown in Fig. 5(f).

Conclusions

A comprehensive understanding of behavioral models and their mechanical properties is essential in the investigation of fractured rock mass stability and the modeling of underground mining pillars. This study utilized Wolfram Mathematica to assess the reliability of mining pillars, with a particular focus on examining the impact of scale and shape on pillar strength. Our analytical approach is grounded in methodologies outlined in the literature review and is firmly based on the Mohr-Coulomb theory.

Our findings provide several key insights:

1. **Effect of Shape:** Our study demonstrates a significant relationship between pillar shape, characterized by the width-to-height (*w*/*h*) ratio, and pillar strength. As the w/h ratio exceeds a critical threshold, pillar strength increases exponentially.
2. **Validation of Size Effect:** Our results confirm the well-documented 'volume or size effect,' where strength decreases with increasing pillar volume. Notably, our Mathematica-based algorithm rigorously evaluates shear potential at each failure plane within the pillar.
3. **Influence of Crack Density:** We observed a complex relationship between crack density and strength. Strength diminishes with increasing volume until a specific threshold is reached, beyond which the decline stabilizes.
4. **Critical Mesh Size and Discretization Effect:** A key finding is identifying a critical mesh size that leads to the weakest pillar behavior and the lowest strength. This highlights the importance of considering mesh size in pillar design and stability assessments. Larger mesh sizes can increase pillar strength but also decrease the number of meshes within a given volume. This reduction occurs because our strength calculation method relies on planes within these meshes, and as the number of meshes decreases, their

orientation tends to align with the internal friction angle, which is associated with the highest strength value.

The reproduction of the scale effect using our Mathematica-based algorithm was aimed at facilitating probabilistic studies due to the random nature of discontinuities in rock masses. Future work should focus on stochastic modeling of fracture networks and their influence on rock mass strength to further enhance our understanding.

References

Alejano, L.R., Arzúa, J., Pérez-Rey, I., 2015. EFFECT OF SCALE AND STRUCTURE ON THE STRENGTH AND DEFORMABILITY OF ROCKS 10.

Alonso, E.E., Tapias, M., Gili, J., 2012. Scale effects in rockfill behaviour. Géotechnique Letters 2, 155–160. https://doi.org/10.1680/geolett.12.00025

Bieniawski, Z.T., 1968. The effect of specimen size on compressive strength of coal. International Journal of Rock Mechanics and Mining Sciences & Geomechanics Abstracts 5, 325–335. https://doi.org/10.1016/0148-9062(68)90004-1

Brady, B.G.H., Brown, E.T., 2004. Rock Mechanics: For Underground Mining. Springer Science & Business Media.

Cheikhaoui, Y, Bensehamdi, S., Cheniti, H., Kanli, A.I., Benselhoub, A., 2021. New formula for evaluation of strength pillar in the underground mine of Chaabet El-Hamra (Setif, Algeria) 53, 12.

Cheikhaoui, Youcef, Deck, O., Omraci, K., Cheniti, H., 2021. The Scale and Shape Effects on the Characteristic Strength of a Rock Mass: Application to Mining Pillars, in: Abdel Wahab, M. (Ed.), Proceedings of 1st International Conference on Structural Damage Modelling and Assessment. Springer Singapore, Singapore, pp. 295–302. https://doi.org/10.1007/978-981-15-9121-1_23

Cundall, P., Pierce, M., Mas Ivars, D., 2008. Quantifying the Size Effect of Rock Mass Strength, in: Proceedings of the First Southern Hemisphere International Rock Mechanics Symposium. Presented at the First Southern Hemisphere International Rock Mechanics Symposium, Australian Centre for Geomechanics, Perth, pp. 3–15. https://doi.org/10.36487/ACG_repo/808_31

Diederichs, M.S., 2002. Stress induced damage accumulation and implications for hard rock engineering. Toronto, pp. 3–12.

Gao, M., Liang, Z., Li, Y., Wu, X., Zhang, M., 2018. End and shape effects of brittle rock under uniaxial compression. Arab J Geosci 11, 614. https://doi.org/10.1007/s12517-018-3957-9

Greminger, M., 1982. Experimental studies of the influence of rock anisotropy on size and shape effects in point-load testing. International Journal of Rock Mechanics and Mining Sciences & Geomechanics Abstracts 19, 241–246. https://doi.org/10.1016/0148-9062(82)90222-4

Griffiths, D.V., Fenton, G.A., 2004. Probabilistic Slope Stability Analysis by Finite Elements. Journal of Geotechnical and Geoenvironmental Engineering 130, 507–518. https://doi.org/10.1061/(ASCE)1090-0241(2004)130:5(507)

Griffiths, D.V., Fenton, G.A., Lemons, C.B., 2002a. Probabilistic analysis of underground pillar stability. International Journal for Numerical and Analytical Methods in Geomechanics 26, 775–791. https://doi.org/10.1002/nag.222

Hoek, E., Brown, E.T., 1997. Practical estimates of rock mass strength. International Journal of Rock Mechanics and Mining Sciences 34, 1165–1186.

Hudson, J., Crouch, S., Fairhurst, C., 1972. Soft, stiff and servo-controlled testing machines: a review with reference to rock failure. Eng Geol 6, 155–189. https://doi.org/10.1016/0013-7952(72)90001-4.

Liu, C.Y., Yang, J.X., Wu, F.F., 2015. A Proposed Method of Coal Pillar Design, Goaf Filling, and Grouting of Steeply Inclined Coal Seams Under Water-Filled Strata. Mine Water Environ 34, 87–94. https://doi.org/10.1007/s10230-014-0314-4

Lunder, P.J., Pakalnis, R.C., 1997a. Determination of the strength of hard-rock mine pillars. CIM Bulletin 90, 51–55.

Lunder, P.J., Pakalnis, R.C., 1997b. Determination of the strength of hard-rock mine pillars. CIM Bulletin 90, 51–55.

Ma, H., Wang, J., Wang, Y., 2012. Study on mechanics and domino effect of large-scale goaf cave-in. Safety Science 50, 689–694.

Martin, C.D., Maybee, W.G., 2000. The strength of hard-rock pillars. International Journal of Rock Mechanics and Mining Sciences 37, 1239–1246. https://doi.org/10.1016/S1365-1609(00)00032-0

Maybee, W.G., 2000. PILLAR DESIGN IN HARD BRITTLE ROCKS. Laurentian University, Sudbury, Ontario, Canada.

Medhurst, T.P., Brown, E.T., 1998. A study of the mechanical behaviour of coal for pillar design. International Journal of Rock Mechanics and Mining Sciences 35, 1087–1105. https://doi.org/10.1016/S0148-9062(98)00168-5

Salamon, M.D.G., 1996. Coal pillar strength from back-calculation: strata control for coal mine design. The University of New South Wales, the Department of Mining Engineering, Sydney.

Wang, P., Yang, T., Xu, T., Cai, M., Li, C., 2016. Numerical analysis on scale effect of elasticity, strength and failure patterns of jointed rock masses. Geosci J 20, 539–549. https://doi.org/10.1007/s12303-015-0070-x

Weibull, W., 1951. A statistical distribution function of wide applicability. ASME Journal of applied mechanics 293–297.

Wolfram Research, Inc, 2023. Mathematica.

York, G., Canbulat, I., 1998. The scale effect, critical rock mass strength and pillar system design. Journal of the Southern African Institute of Mining and Metallurgy 98, 23–37.

Yoshinaka, R., Osada, M., Park, H., Sasaki, T., Sasaki, K., 2008. Practical determination of mechanical design parameters of intact rock considering scale effect. Engineering Geology 96, 173–186. https://doi.org/10.1016/j.enggeo.2007.10.008

Zhang, Q., Zhu, H., Zhang, L., Ding, X., 2011. Study of scale effect on intact rock strength using particle flow modeling. International Journal of Rock Mechanics and Mining Sciences 48, 1320–1328. https://doi.org/10.1016/j.ijrmms.2011.09.016

Zipf, R.K., Mark, C., 1997. Design methods to control violent pillar failures in room-and-pillar mines. Transactions of the Institution of Mining and Metallurgy-Section A-Mining Industry 106.